Geochemistry Geophysics Geosystems G3
AN ELECTRONIC JOURNAL OF THE EARTH SCIENCES
Published by AGU and the Geochemical Society

Article
Volume 8, Number 2
20 February 2007
Q02009, doi:10.1029/2006GC001442
ISSN: 1525-2027

REMAP: A reaction transport model for isotope ratio calculations in porous media

Boris M. Chernyavsky and Ulrich G. Wortmann

Geobiology Isotope Laboratory, Department of Geology, University of Toronto, 22 Russell Street, Toronto, Ontario, Canada M5S 3B1 (chernyavsky@geology.utoronto.ca)

[1] Reactive transport modeling has become an important tool in geochemistry and has recently been expanded to isotopic studies as well. However, there is currently no publicly available code specifically tailored to isotopic studies. We therefore present here a computer program for 1-D reactive transport modeling of bacterially mediated isotope fractionation processes in porous media. Our numerical method allows the modeling of both stationary and time-dependent processes and implements various boundary condition types, including floating boundaries. The model specifically handles cases where the substrate is fully consumed, either at the lower boundary or at any point within the model. We provide a detailed analysis of our implementation as well as some example cases. The program is designed to be run on Matlab or Octave, which are available for all major operating systems.

Components: 895 words, 4 figures.

Keywords: numerical modeling; reactive transport; bacterially mediated isotope fractionation.

Index Terms: 0560 Computational Geophysics: Numerical solutions (4255); 1051 Geochemistry: Sedimentary geochemistry; 4805 Oceanography: Biological and Chemical: Biogeochemical cycles, processes, and modeling (0412, 0414, 0793, 1615, 4912).

Received 4 August 2006; **Revised** 6 November 2006; **Accepted** 22 November 2006; **Published** 20 February 2007.

Chernyavsky, B. M., and U. G. Wortmann (2007), REMAP: A reaction transport model for isotope ratio calculations in porous media, *Geochem. Geophys. Geosyst.*, *8*, Q02009, doi:10.1029/2006GC001442.

1. Introduction

[2] Reaction transport modeling of chemical reactions in porous media is a common approach for the interpretation of geochemical data, and has long been used to model diagenetic reactions in marine sediments [e.g., *Berner*, 1980; *Dhakar and Burdige*, 1996; *Cappellen and Wang*, 1996; *Boudreau*, 1996; *Soetaert et al.*, 1996; *Wijsman et al.*, 2002; *Rysgaard and Berg*, 1996; *Luff et al.*, 2000; *Meysman et al.*, 2005; *Berg et al.*, 2003; *Wortmann*, 2006]. Due to its usefulness, a variety of model codes are available [see *Middelburg et al.*, 2003, and references therein]. While reaction transport modeling has the potential to significantly contribute to isotopic studies, the number of studies is more limited [e.g., *Jørgensen*, 1979; *Rudnicki et al.*, 2001; *Wortmann et al.*, 2001; *Böttcher et al.*, 2004], and no generally available computer model does exist.

[3] Therefore the primary aim of our article is to present a program which allows modeling of bacterially mediated consumption of a substrate and the associated isotopic effects on the substrate and product using a variety of boundary conditions. The model is written in Matlab/Octave code and as

such targeted to researchers with a less extensive background in numerical modeling. As it has been pointed out by several authors [e.g., *Sasowsky*, 2006], numerical models must be reproducible by other scientists and validated against a set of known cases. To this end we provide a detailed description of the algorithm, its assumptions and limitations, and a set of validation cases which can be reproduced by other scientists. The program, a user guide, and examples are available as auxiliary material[1] to this publication (see Software S1).

2. Methods

[4] In this study we investigate the distribution of dissolved chemical species modified by bacterial activity in a porous medium (i.e., marine sediments). We refer to the species which is consumed as the substrate, and the species which is produced as the product. Both, substrate and product are also affected by diffusion and potentially advection. Such a system can be modeled if we know the diffusion coefficients of a given species, the overall advection velocity, and the reaction rate at a given depth. Boundary conditions in marine sediments typically include fixed concentration values (a so-called Dirichlet condition) at the upper boundary, as the overlying ocean water is in most cases an infinite reservoir. The lower boundary condition can also be either given as a concentration (a Dirichlet condition), or the concentration gradient (a so-called Neumann condition). The latter condition is especially useful in cases were a species becomes extinct at depth, but there is no a priory knowledge of the extinction depth. We will further refer to such a combination of a Neumann and Dirichlet condition as "free" or "floating" boundary condition.

[5] In the following, we choose the sediment-water interface to be our reference frame. This implies that the water buried during the sedimentation process moves downward relative to the chosen coordinate system, despite the fact that compaction results in an upward movement relative to the individual sediment layer (for a detailed discussion, see *Berner* [1980]).

[6] Biologically mediated reactions in marine sediments are commonly described by the standard 1-D diagenetic equation [*Berner*, 1980]

$$\frac{\partial(\phi C)}{\partial t} = \frac{\partial}{\partial z}\left(D_B \frac{\partial(\phi C)}{\partial z} + \phi(D_i + D)\frac{\partial C}{\partial z}\right) - \frac{\partial \phi \omega C}{\partial z} - \phi f \tag{1}$$

where C is the concentration of the substrate, t is time, ϕ is the porosity, D is the diffusivity coefficient, D_B is the bioturbation coefficient, D_i is the irrigation coefficient, ω is the advective velocity relative to the chosen coordinate system and f is the reactive term describing the consumption of the substrate and production of the product.

[7] In the following, we will assume that bioturbation and irrigation are absent and that sedimentation is a steady process. We further assume that porosity changes are due to the compaction process alone (i.e., $\frac{\partial \phi}{\partial t} = 0$; for a more involved discussion, see *Berner* [1980] and *Meysman et al.* [2005]). This allows us to simplify equation (1) as

$$\frac{\partial C}{\partial t} = \frac{\partial C}{\partial z}\frac{\partial D}{\partial z} + D\frac{\partial^2 C}{\partial z^2} + \frac{D}{\phi}\frac{\partial C}{\partial z}\frac{\partial \phi}{\partial z} - \omega\frac{\partial C}{\partial z} - f \tag{2}$$

where $\omega = \omega_s + \omega_f$ is a sum of the externally impressed flow velocity ω_f, and the downward directed velocity ω_s caused by burial adjusted for compaction.

[8] Equation (2) applies also to the distribution of isotopic species, but since bacteria may discriminate between different isotopes, the reaction term f has to be modified for each isotope accordingly. Here we follow the notion proposed by *Jørgensen* [1979] and write

$$f_A = \frac{\alpha C_A}{C + (\alpha - 1)C_A} f \tag{3}$$

and

$$f_B = \frac{C_B}{\alpha C - (\alpha - 1)C_B} f \tag{4}$$

where A denotes the light isotope, B denotes the heavy isotope, and α the fractionation factor. In a zero-dimensional case, α can be related to the isotopic enrichment factor ϵ which describes the isotopic difference of the substrate entering the cell and the product leaving the cell, and we can write

$$\alpha = 1 - \frac{\delta^X C_P - \delta^X C_S}{1000} \tag{5}$$

[1] Auxiliary materials are available in the HTML. doi:10.1029/2006GC001442.

where $\delta^X C_P$ is the delta value of the product, and $\delta^X C_S$ is the delta value of the substrate. The delta value represents the ratio between 2 isotopes as

$$\delta^X C = \left(\frac{\frac{C_B}{C_A}}{R} - 1 \right) \times 1000 \quad [‰] \tag{6}$$

where R is the ratio of C_A and C_B in the respective standard material.

[9] Many biological processes are dependent on substrate concentration. Bacterially mediated sulfate reduction, e.g., is limited for sulfate concentrations below 0.2 mM [*Habicht et al.*, 2002]. We model this substrate dependence using a special case of Michaelis-Menten kinetics, using a so called Monod-type limiter in the reaction term f

$$f = g \frac{C}{L + C} \tag{7}$$

where L is the substrate concentration value at which metabolic activity has dropped to 50% [see also *Boudreau and Westrich*, 1984]. Experimental results [*Habicht et al.*, 2005] and theoretical considerations [*Brunner and Bernasconi*, 2005] suggest that α also depends on substrate concentration, which we implement in a similar way

$$\alpha = 1 + \alpha_0 \frac{C}{L_\alpha + C} \tag{8}$$

where L_α is a limiter [see, e.g., *Habicht et al.*, 2005] similar to L but applied to the fractionation factor rather than to the reduction function, and α_0 is initial fractionation factor in the region of high substrate concentration. The user is free to choose the limiter values, and a value of zero will disable this feature altogether.

2.1. Numerical Implementation

[10] While explicit code schemes are easy to implement, they have stringent stability criteria and are computationally inefficient. Implicit schemes on the other hand are complicated to implement if the reaction term is non-linear. A number of alternative approaches using operator splitting, such as the Sequential Non-Iterative Approach (SNIA) [*Zysset and Stauffer*, 1992], the Strang Splitting [*Strang*, 1968] and the Sequential Iteration Approach (SIA) [*Yeh and Tripathi*, 1989; *Zysset and Stauffer*, 1992] were proposed, which significantly simplify the implementation while preserving reasonable accuracy [see also *Steefel and MacQuarrie*, 1996].

[11] Here we choose a second order accurate semi-implicit numerical scheme for solving this equation. The term "semi-implicit" refers to the implicit treatment of the transport, diffusion and advection terms and the explicit treatment of the reaction term. The semi-implicit method used in the present study provides an accurate solution with a relatively simple implementation at the expense of a small increase in the convergence time, and a loss of absolute stability. The method was tested against an explicit solver, and against a fully implicit solver with non-linear terms linearized through Taylor decomposition [*Fletcher*, 1991]. The semi-implicit method provides accurate solutions and fast convergence for steady state problems and most unsteady problems. A degraded convergence can be encountered in the case of a time-dependent solution with very fast transport, and the stability conditions may require the decrease of the time step under certain conditions.

[12] We use the following universal scheme:

$$(1 + \gamma) \frac{\Delta C_j^{n+1}}{\Delta t} - \gamma \frac{\Delta C_j^n}{\Delta t} = (1 - \beta) R_j^n + \beta R_j^{n+1} \tag{9}$$

where the upper index ("n") refers to the time step, the lower index ("j") refers to the spatial step, R denotes the right hand side of equation (2) after simplification and $\Delta C_j^n = C_j^n - C_j^{n-1}$. The scheme becomes an implicit scheme with $\beta = 1$, $\gamma = 0$, a Crank-Nicholson scheme with $\beta = \frac{1}{2}$, $\gamma = 0$, and a three layer purely implicit scheme with $\beta = 1$, $\gamma = \frac{1}{2}$. For comparison we can also run our code as an explicit scheme by using $\beta = 0$, $\gamma = 0$. Both the Crank-Nicholson scheme and the three-layer purely implicit scheme are second order accurate in time for time-dependent solutions. This gives us additional flexibility to choose a scheme with appropriate properties for a given problem. Aside from being more accurate in time, the Crank-Nicholson scheme is well known to provide more accurate and less diffusive solutions, particularly in cases with high gradients [*Fletcher*, 1991]. However, it is also known to produce oscillatory solutions, particularly with stiff systems, i.e., systems in which physical processes exhibit strongly distinguishing temporal characteristics. In this case an application of the three-layer pure implicit scheme results in a more well-behaved solution while still preserving a higher order of accuracy than the implicit scheme. While high order schemes offer little advantage for solution of steady-state problems and require significantly more iterations to converge, we have found them

useful in the solution of the time-dependent problems.

[13] We can now proceed with the discretization of equation (2) as follows:

$$\begin{aligned}
&(1+\gamma)\frac{C_j^{n+1}-C_j^n}{\Delta t}-\gamma\frac{C_j^n-C_j^{n-1}}{\Delta t}\\
&=(1-\beta)\frac{C_{j+1}^n-C_{j-1}^n}{2\Delta z}\frac{D_{j+1}-D_{j-1}}{2\Delta z}\\
&\quad+(1-\beta)D_j\frac{C_{j+1}^n-2C_j^n+C_{j-1}^n}{\Delta z^2}\\
&\quad+(1-\beta)\frac{D_j}{\phi_j}\frac{C_{j+1}^n-C_{j-1}^n}{2\Delta z}\frac{\phi_{j+1}-\phi_{j-1}}{2\Delta z}\\
&\quad+\beta\frac{C_{j+1}^{n+1}-C_{j-1}^{n+1}}{2\Delta z}\frac{D_{j+1}-D_{j-1}}{2\Delta z}\\
&\quad+\beta D_j\frac{C_{j+1}^{n+1}-2C_j^{n+1}+C_{j-1}^{n+1}}{\Delta z^2}\\
&\quad+\beta\frac{D_j}{\phi_j}\frac{C_{j+1}^{n+1}-C_{j-1}^{n+1}}{2\Delta z}\frac{\phi_{j+1}-\phi_{j-1}}{2\Delta z}\\
&\quad-(1-\beta)\omega_j\frac{C_{j+1}^n-C_{j-1}^n}{2\Delta z}\\
&\quad-\beta\omega_j\frac{C_{j+1}^{n+1}-C_{j-1}^{n+1}}{2\Delta z}-f_j
\end{aligned}\tag{10}$$

Note that we use central differences for the discretization of the first and second order derivatives [*Crank*, 1975; *Roache*, 1982]. This allows us to keep the second order of accuracy in space, but may result in oscillatory solutions [*Boudreau*, 1997; *Fletcher*, 1991]. In order to avoid the spatial oscillations, the cell Reynolds number (or Péclet number) limit $R_{cell}=\frac{\omega\Delta z}{D}<2$ must be observed for central differences [*Fletcher*, 1991]. It is, however, possible to eliminate this limitation altogether by replacing the central difference with weighted, or blended upstream and central differences, which eliminates oscillatory behavior while preserving second order accuracy in space [*Fiadeiro and Veronis*, 1977].

[14] By regrouping the terms of equation (10) for C_{j-1}, C_j and C_{j-1} we obtain

$$a_jC_{j+1}^{n+1}+b_jC_j^{n+1}+c_jC_{j-1}^{n+1}=d_j \tag{11}$$

where

$$a_j=\frac{\beta}{2\Delta z}\frac{D_{j+1}-D_{j-1}}{2\Delta z}+\frac{\beta D_j}{\Delta z^2}+\frac{\beta D_j}{\phi_j 2\Delta z}\frac{\phi_{j+1}-\phi_{j-1}}{2\Delta z}-\frac{\beta\omega_j}{2\Delta z} \tag{12}$$

$$b_j=\frac{2\beta D_j}{\Delta z^2}-\frac{1+\gamma}{\Delta t} \tag{13}$$

$$c_j=-\frac{\beta}{2\Delta z}\frac{D_{j+1}-D_{j-1}}{2\Delta z}+\frac{\beta D_j}{\Delta z^2}-\frac{\beta D_j}{\phi_j 2\Delta z}\frac{\phi_{j+1}-\phi_{j-1}}{2\Delta z}+\frac{\beta\omega_j}{2\Delta z} \tag{14}$$

$$\begin{aligned}
d_j=&-(1+2\gamma)\frac{C_j^n}{\Delta t}+\gamma\frac{C_j^{n-1}}{\Delta t}\\
&-(1-\beta)\frac{C_{j+1}^n-C_{j-1}^n}{2\Delta z}\frac{D_{j+1}-D_{j-1}}{2\Delta z}\\
&-(1-\beta)D_j\frac{C_{j+1}^n-2C_j^n+C_{j-1}^n}{\Delta z^2}\\
&-(1-\beta)\frac{D_j}{\phi_j}\frac{C_{j+1}^n-C_{j-1}^n}{2\Delta z}\frac{\phi_{j+1}-\phi_{j-1}}{2\Delta z}\\
&+(1-\beta)\omega_j\frac{C_{j+1}^n-C_{j-1}^n}{2\Delta z}+f_j
\end{aligned}\tag{15}$$

We can write this equation for all $j=2\ldots N-1$, where N is the number of the grid points, obtaining a set of $N-2$ linear equations, which together with the boundary conditions can be presented in matrix form as

$$\begin{pmatrix} b_{ub} & c_{ub} & 0 & \ldots & \\ & & \ldots & & \\ 0 & a_j & b_j & c_j & 0 \\ & & \ldots & & \\ & \ldots & 0 & a_{lb} & b_{lb} \end{pmatrix}\begin{pmatrix} C_1 \\ \ldots \\ C_j \\ \ldots \\ C_N \end{pmatrix}=\begin{pmatrix} d_{ub} \\ \ldots \\ d_j \\ \ldots \\ d_{lb} \end{pmatrix} \tag{16}$$

where b_{ub}, c_{ub}, d_{ub}, a_{lb}, b_{lb}, and d_{lb} are determined by the upper and lower boundary conditions respectively. The inversion of this matrix yields the solution for this equation system.

2.2. Boundary Conditions

[15] To complete the matrix we need to formulate the boundary conditions which will give us the values of the matrix coefficients b_{ub}, c_{ub}, d_{ub}, a_{lb}, b_{lb}, and d_{lb}. Since the variables are usually known at the upper boundary we use a simple Dirichlet condition, which corresponds to the choice of $b_{ub}=1$, $c_{ub}=0$ and $d_{ub}=C_{upper\text{-}boundary}$.

[16] In our model we consider three types of lower boundary condition: (1) the Dirichlet boundary condition at a known depth, similar to the upper boundary which can be used in cases when the substrate concentration at the lower boundary is known [e.g., *Wortmann*, 2006], (2) Neumann boundary condition at the known depth, and (3) the Neumann condition set at the a priori unknown depth (“free boundary”) [*Boudreau and Westrich*, 1984]. The latter case is of interest for a variety of cases, e.g., when a Dirichlet condition would over-determine the system. In

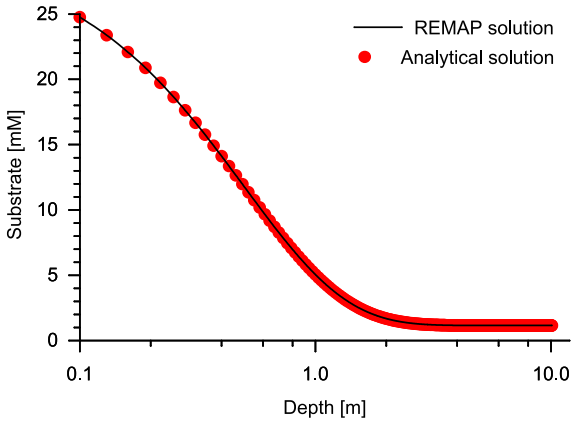

Figure 1. Comparison of analytical and numerical derived solutions.

other cases, it may be of interest to explore how the system would behave below the last known data point, or to explore the theoretical behavior of a system without a priori knowledge of the location of the lower boundary or the concentration at this boundary [see, e.g., *Wortmann and Chernyavsky*, 2007]. Last but not least, a chemical species may be supplied from both above and below, but become extinct in between [e.g., *Rudnicki et al.*, 2001; *Böttcher et al.*, 2004]. While this latter case can be modeled with two independent models, it would be convenient to be able to model this situation in a single run.

[17] If the concentration at (or the location of) the lower boundary is not known, we can formulate the following condition:

$$\left.\frac{\partial C}{\partial z}\right|_{z=z_{lb}} < \epsilon_{grad} \tag{17}$$

where ϵ_{grad} is a gradient sufficiently small to be considered negligible, i.e., we solve our equation system until the substrate concentration value would reach an essentially constant value. This still leaves us with an unknown depth z_{lb} where this condition is applied, and which needs to be defined independently. In most cases we can either assume that all the substrate is eventually consumed or that all consumption eventually stops. Thus we can write an additional condition where

$$C = Const|_{z=z_{lb}} \tag{18}$$

[18] Now the number of unknowns matches the number of independent equations and the problem becomes well posed and can be solved numerically using an iterative approach. We first use a Dirichlet condition at the lower boundary to obtain an initial guess for the location of z_{lb}. We then compare the gradient at the lower boundary with ϵ_{grad} and proceed to move the location of z_{lb} toward the surface or further down from the surface with a step size Δz until the gradient exceeds ϵ_{grad}. If the gradient becomes smaller than ϵ_{grad} (in case our initial guess of the complete consumption depth was too shallow) we reverse the sign and reduce the value of Δz until we converge to the location where $C = 0$ and $\frac{\partial C}{\partial z} < \epsilon_{grad}$ with an accuracy of ϵ_z. This procedure proves to be efficient and quick to converge.

[19] Note, however, that in cases where the substrate is fully consumed at the lower boundary numerical solvers may have difficulties to converge if the user selects the wrong time step. *Boudreau and Westrich* [1984] suggested therefore to use a concentration-dependent limiter for the reduction term, which greatly increases numerical stability. Our model therefore provide parameters to set independent limiters for the fractionation factor and the consumption function. However, we caution users of our model to carefully consider whether the use of limiters is physical or not (see also the discussion of limiters in section 2).

2.3. Validation

[20] We validated our model by comparing the output of REMAP with the output of alternative solvers and against two analytical solutions. In the first case we investigated how our solver compares against a steady state problem with an idealized power law substrate reduction function (taken from *Boudreau* [1997])

$$D\frac{d^2C}{dz^2} - \omega\frac{dC}{dz} - \chi\exp(-\xi z) = 0 \tag{19}$$

$$C(0) = C_0 \tag{20}$$

$$\left.\frac{dC}{dz}\right|_{x\to\infty} = 0 \tag{21}$$

which can be solved as

$$C(z) = C_0 + \frac{\chi}{D\xi^2 + \omega\xi} - \frac{\chi\exp(-\xi z)}{D\xi^2 + \omega\xi} \tag{22}$$

where $\chi = 6 \times 10^{-8}$ mM/s and $\xi = 2$ m^{-1} are model coefficients, $D = 5 \times 10^{-10}$ m^2/s, $\omega = 4 \times 10^{-9}$ m/s, and the upper boundary condition is $C_0 = 30$ mM. Figure 1 shows that the numerical and analytical solution are identical.

[21] In the second case, we investigated how well REMAP locates the extinction depth, by calculating the theoretical extinction depth from

$$D\frac{d^2C}{dz^2} - \zeta = 0 \tag{23}$$

$$C(0) = C_0 \tag{24}$$

$$C(L) = 0 \tag{25}$$

$$\left.\frac{dC}{dL}\right|_L = 0 \tag{26}$$

where L is the extinction depth (in m), which can be solved as

$$L = \sqrt{\frac{2DC_0}{\zeta}} \tag{27}$$

$$C(z) = \frac{\zeta z^2}{2D} - \frac{\zeta L}{D}z + C_0 \tag{28}$$

where $\zeta = 8 \times 10^{-7}$ mM/s is a zeroth order reduction function.

[22] The analytically and numerically computed locations where the substrate is entirely consumed differ by 1×10^{-4} m which is identical to the grid resolution (i.e., cell size) of the model. We additionally compare the results obtained by an explicit and fully implicit (utilizing Taylor linearization) solver and observe good agreement between the solutions.

2.4. Parametric Study and Convergence Analysis

[23] Convergence behavior of a given problem should be considered for each problem independently. We nevertheless subjected our model to a parametric study to test that it successfully handles typical conditions. We modified α from 0 to 100‰, using upper boundary concentrations from 30 to 1 mM, and advection rates from -1×10^{-10} m/s (with imposed external velocity) to 1×10^{-10} m/s, using a fixed sedimentation rate of 6×10^{-11} m/s. All runs use a power-law type reduction function ($g = 0.00205e^{-6}/2 \times (z/1.5113 + 0.1)^{-2.15}$) with reaction term limiters from 0.01 to 1.0 mM. We used a 1000 point grid resolution and a zero-gradient free lower boundary condition as a baseline. REMAP converged for all runs within these boundaries. However, as Figure 2a shows, convergence alone does not guarantee a correct solution, which can be also dependent on the grid resolution. Isotopic offsets because of improper grid resolution may be as high as 30‰. Note that the case illustrated in Figure 2 used a significant upward advection velocity (externally imposed $\omega = -12 \times 10^{-11}$ m/s) to emphasize the influence of resolution and convergence criteria.

[24] An important choice in each model is the criterion used to determined whether a solution has been achieved or whether further computation is necessary. We chose to utilize a dimensional convergence criteria for concentrations

$$\frac{1}{N}\sum_{j=1}^{N}|C_j^n - C_j^{n-1}| < \epsilon_{conv}, \tag{29}$$

and for isotope ratios we define

$$\frac{1}{N}\sum_{j=1}^{N}|\delta^X C_j^n - \delta^X C_j^{n-1}| < \epsilon_{dc}, \tag{30}$$

where C_j^n and C_j^{n-1} are concentration values, and $\delta^X C_j^n$ and $\delta^X C_j^{n-1}$ are isotope ratios. The influence of ϵ_{conv} on the result of the computation is shown Figure 2b. Note, however, that the accurate solution for the total concentration does not guarantee an equally accurate solution for the isotope ratio, since it depends on the ratio of the concentration values which can themselves be rather small near the extinction point, which requires that $\epsilon_{dc} < \epsilon_{conv}$.

3. Usage and Examples

[25] The model is written using the Matlab/Octave language for which most universities will offer training courses. It will run on any Matlab or Octave equipped computer independent of operating system or hardware. The model is driven by an input file which specifies the model setup, the name of files holding auxiliary data, the name of output files, etc. All units are standard SI units, (i.e., m, s, mol), except for the temperature measured in degrees Celsius. The input file parser can handle simple equations, and will automatically interpolate input data to the required grid-resolution. For the following examples, we provide input files as starting point to the interested user. For details on the input file format, see the user guide and the annotated example files in the auxiliary material (Software S1).

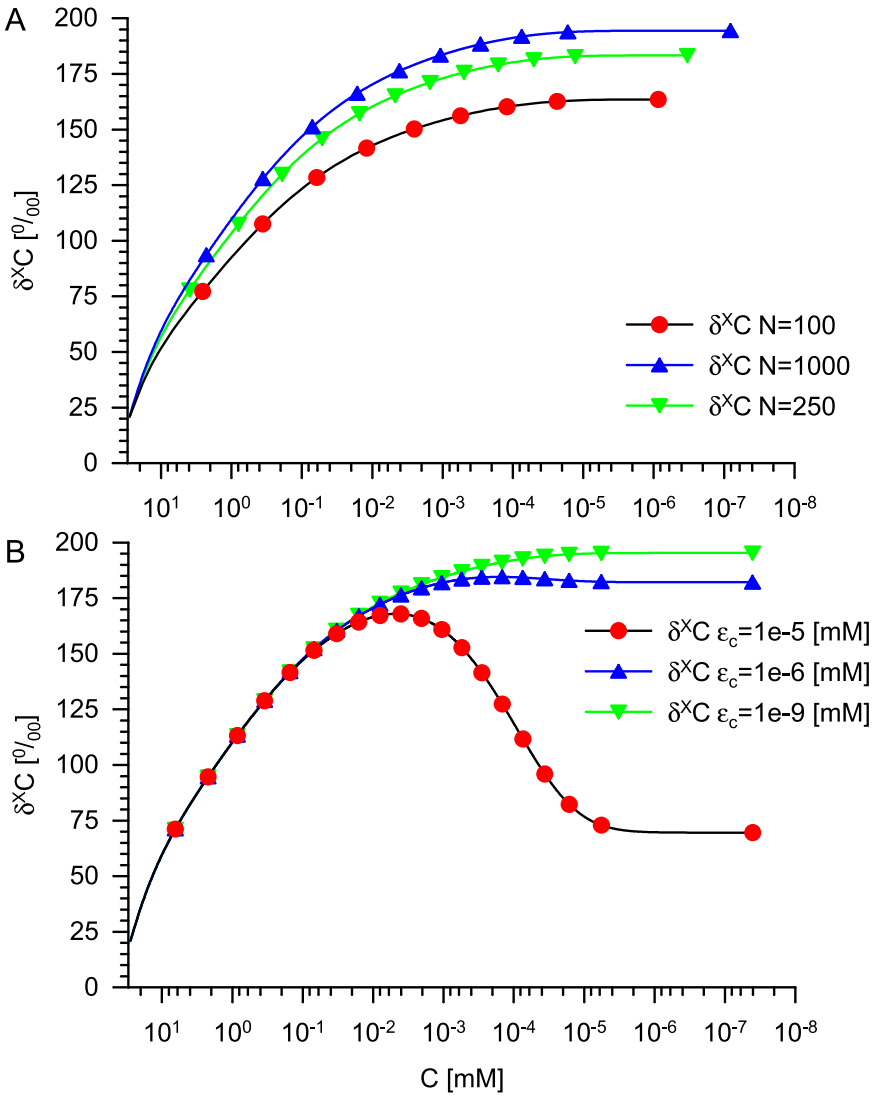

Figure 2. (a) Influence of the grid resolution on the computed isotope ratio. The effect of lower grid resolutions is mainly visible for concentrations below 1 mM. (b) Evolution of the isotopic ratio versus concentration (depth) for different convergence criteria. It is apparent that the correctness of the solution depends heavily on the chosen convergence criterion. Note that the above model was run with a substrate concentration independent fractionation factor $\alpha = 1.065‰$, a sedimentation rate 6×10^{-11} m/s, and imposed advection velocity $\omega = -12 \times 10^{-11}$ m/s with the following reduction function: $g = 0.00205e^{-6}/2 \times (z/1.5113 + .1)^{-2.15}$, using a limiter 0.7 for the concentration calculations. Note that the convex shape of the isotope-depth plot is largely a result of the strong upward advection.

3.1. Using a Dirichlet Condition at the Upper and Lower Boundary

[26] *Jørgensen* [1979] investigated the $\delta^{34}S$ distribution in sediments from Limfjorden using a reaction transport model with a Dirichlet condition at the upper and lower boundary. He described his depth-dependent sulfate reduction using an exponential function

$$f = \zeta z^{-\chi} \tag{31}$$

where $\zeta = 0.5 \times 10^{-16}$ [mol/m^3 s^{-1}] and $\chi = 2.15$. Using the above equations, f would be infinity for $z = 0$. *Jørgensen* [1979] therefore modeled his example starting with a depth of 0.15 m. Furthermore, he considered his case to be stationary, and used constant diffusion coefficient and sedimentation rate ($D = 0.4 \times 10^{-11}$ m^2 s^{-1}, $\omega = 0.6 \times 10^{-10}$ ms^{-1}, $\alpha = 1.025$). *Jørgensen* [1979] assumed that 90% of all H_2S is precipitated as pyrite, which is problematic, as he did not implement a proper pyrite model but simply assumed that the reaction term for H_2S decreases

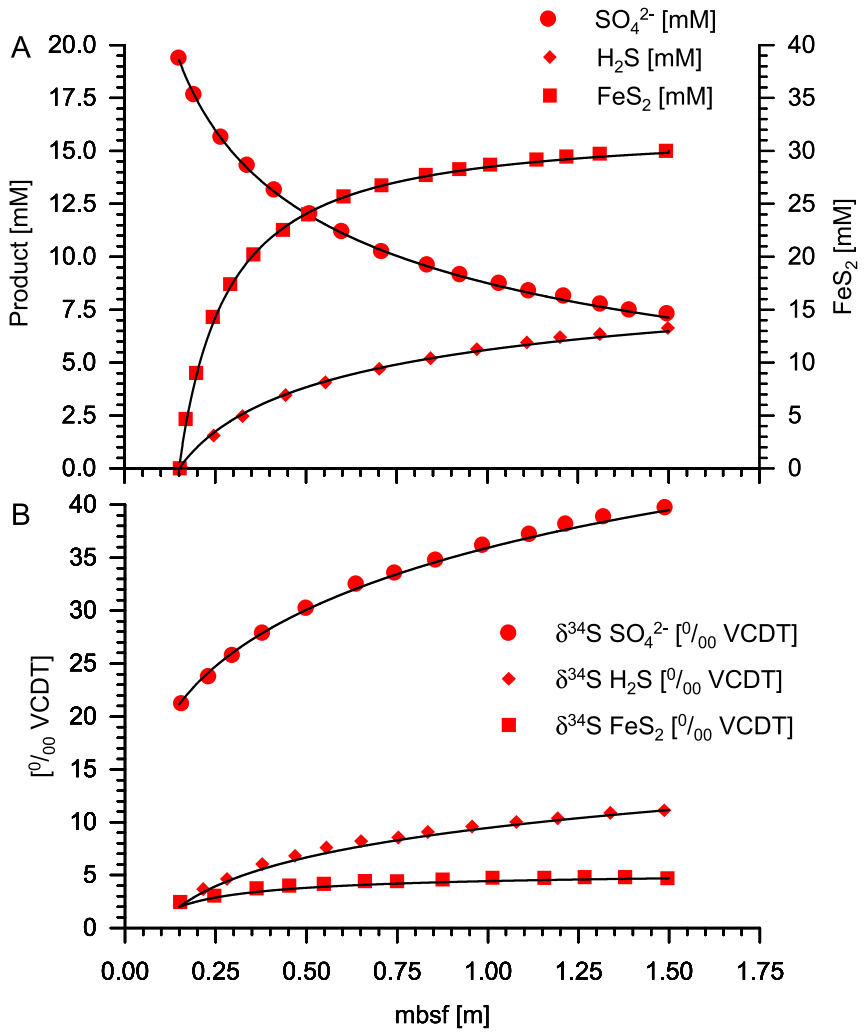

Figure 3. Comparison of the REMAP results with the results published by *Jørgensen* [1979]. Filled circles are data points digitized from *Jørgensen* [1979]; lines are REMAP data.

proportionally. We implemented this approach to be able to compare our results, but discourage the use of this feature. We rerun the case presented by *Jørgensen* [1979] with our model (see the input file joergensen.rmp) and compare our results with the original data in Figure 3.

3.2. Using Auxiliary Data Files

[27] Here we show an example which uses auxiliary files to provide data on substrate consumption, porosity, and temperature. The actual data is from ODP Site 1130 [*Feary et al.*, 2000], which constitutes a 300 m thick succession of Pliocene to Quaternary cool water carbonates [*Feary et al.*, 2000]. Site 1130 is influenced by an upwelling brine, supplying sulfate from below, fueling an unusual ecosystem of sulfate reducing bacteria to a depth of at least 300 mbsf [*Wortmann et al.*, 2001; *Wortmann*, 2006]. This Site is particularly interesting to sulfur isotope studies, as the isotopic difference between dissolved sulfate and dissolved sulfide exceeds 70‰, suggesting a biological mediated isotope effect far greater than previously thought possible [*Rudnicki et al.*, 2001; *Wortmann et al.*, 2001; *Brunner and Bernasconi*, 2005].

[28] To model Site 1130 we first model the distribution of the conservative chloride ion to quantify the vertical advection rate. This is done by setting the reduction function to a constant value of zero, and specifying the velocity of the external flux. As this flux is upward directed, and the origin of our coordinate system is the seafloor, the sign of this velocity must be negative.

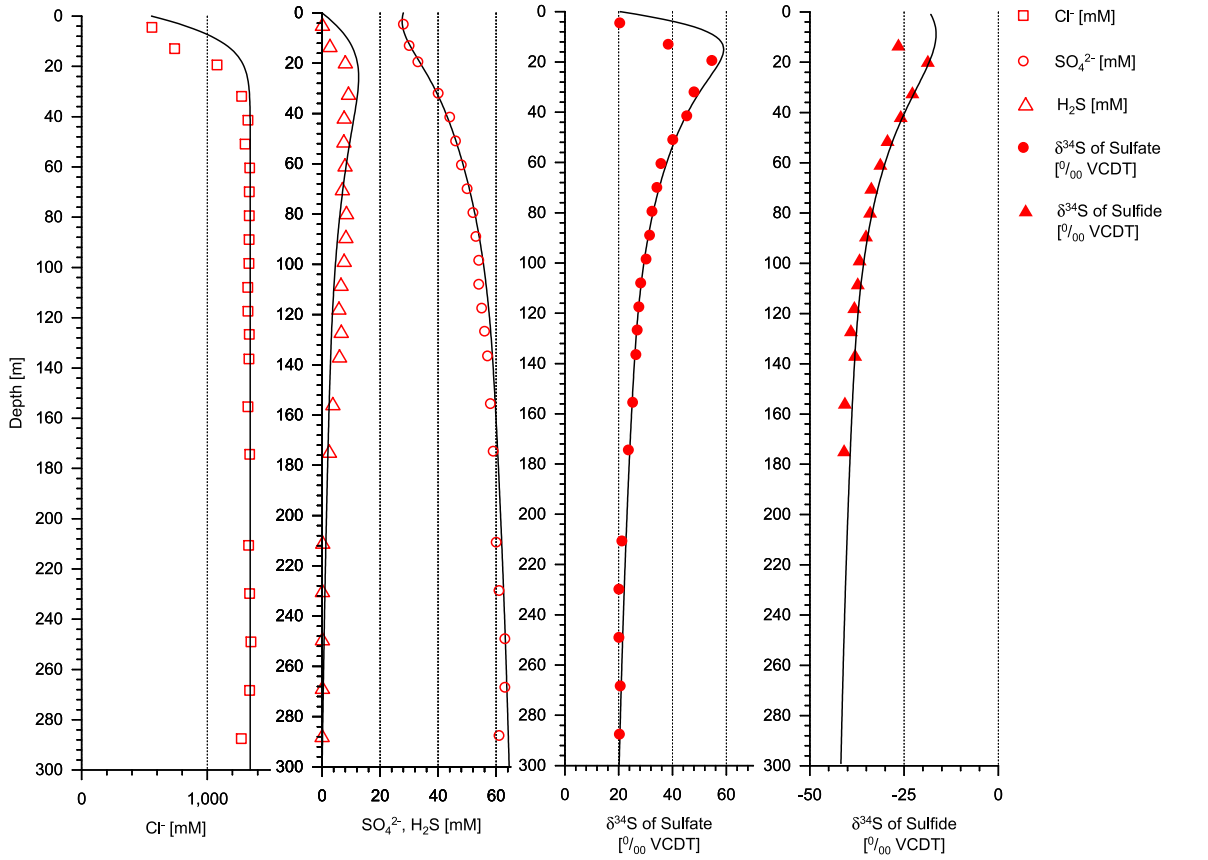

Figure 4. Results of the ODP Site 1130 model. Markers refer to measured data; lines refer to model results. Note that the current REMAP version has no proper pyrite model, and the differences observed in the upper 30 mbsf are caused by an unknown physical process or a result of the steady state compaction assumption. A detailed discussion of the sulfur geochemistry of ODP Site 1130 is given by *Wortmann et al.* [2001] and *Wortmann* [2006].

[29] Here we modify the input file to point to external files holding temperature and porosity data. If the user also specifies the diffusion coefficient using the regression parameters listed by *Boudreau* [1997], the program will automatically calculate the actual diffusion coefficients based on the temperature and porosity data. Note, however, that the current version of REMAP only handles steady state compaction, and that the onus is on the user to provide a porosity file which satisfies this condition.

[30] Figure 4 shows that our results are either much higher than the actually observed values in upper 30 mbsf, or much smaller than the observed values below 30 mbsf. These differences remain if we allow for time-dependent changes in upwelling velocity, and are possibly an artifact of the steady state compaction assumption or caused by an unknown process [*Wortmann*, 2006]. Nevertheless, REMAP successfully models the deeper parts of ODP Site 1130. To match the observed sulfide concentration the model requires that about 50% of all sulfide is converted to pyrite. Note, however, that the current model does not provide a proper pyrite precipitation model, but simply converts a fixed amount of the product phase to pyrite [see *Jørgensen*, 1979]. In the above case we used Dirichlet boundary conditions on the upper and lower boundary. The input files for this simulation are provided in the auxiliary material, and the parameterization of ODP Site 1130 is discussed in detail by *Wortmann et al.* [2001] and *Wortmann* [2006].

4. Summary

[31] We present a numerical code for reactive transport modeling of bacterially mediated processes in porous media which allows us to model isotope fractionation processes for a variety of physical conditions. Our model gracefully handles complete

substrate consumption, accounts for changes in porosity and compaction, and allows for a variety of boundary conditions, including floating boundaries. Various incarnations of this program have previously been used to model cases presented by *Wortmann et al.* [2001], *Böttcher et al.* [2004], and *Wortmann and Chernyavsky* [2007], and we hope that the release of our code is a first step of building a modeling toolkit for marine isotope geochemists.

Acknowledgments

[32] We would like to thank Charly Banks and Pierre-Yves Robin for discussions. The reviews by Bernhard Boudreau and an anonymous reviewer helped to focus this manuscript.

References

Berg, P., S. Rysgaard, and B. Thamdrup (2003), Dynamic modeling of early diagenesis and nutrient cycling: A case study in arctic marine sediment, *Am. J. Sci.*, *303*, 905–955.

Berner, R. A. (1980), *Early Diagenesis: A Theoretical Approach*, Princeton Univ. Press, Princeton, N. J.

Böttcher, M. E., B. Keun-Khim, A. Suzuki, U. G. Wortmann, and H.-J. Brumsack (2004), Microbial sulfate reduction in deep sediments of the southwest Pacific (ODP Leg 181; sites 1119 to 1125): Evidence from stable sulfur isotope fractionation and pore water modeling, *Mar. Geol.*, *205*, 249–260.

Boudreau, B. P. (1996), A method-of-lines code for carbon and nutrient diagenesis in aquatic sediments, *Comput. Geosci.*, *22*, 479–496.

Boudreau, B. P. (1997), *Diagenetic Models and Their Implementation*, Springer, New York.

Boudreau, B. P., and J. T. Westrich (1984), The dependence of bacterial sulfate reduction on sulfate concentration in marine sediments, *Geochim. Cosmochim. Acta*, *48*, 2503–2516.

Brunner, B., and S. M. Bernasconi (2005), A revised isotope fractionation model for dissimilatory sulfate reduction in sulfate reducing bacteria, *Geochim. Cosmochim. Acta*, *69*, 4759–4771.

Cappellen, P. V., and Y. Wang (1996), Cycling of iron and manganese in surface sediments: A general theory for the coupled transport and reaction of carbon, oxygen, nitrogen, sulfur, iron and manganese, *Am. J. Sci.*, *296*, 197–243.

Crank, J. (1975), *The Mathematics of Diffusion*, Oxford Univ. Press, New York.

Dhakar, S. P., and D. J. Burdige (1996), A coupled, non-linear, steady state model for early diagenetic processes in pelagic sediments, *Am. J. Sci.*, *296*, 296–330.

Feary, D. A., et al. (2000), *Proceedings of the Ocean Drilling Program, Initial Reports* [CD-ROM], vol. 182, Ocean Drill. Program, College Station, Tex.

Fiadeiro, M. E., and G. Veronis (1977), On weighted-mean schemes for the finite difference approximation to the advection-diffusion equation, *Tellus*, *29*, 512–522.

Fletcher, C. A. J. (1991), *Computational Techniques for Fluid Dynamics*, Springer, New York.

Habicht, K. S., M. Gade, B. Thamdrup, P. Berg, and D. E. Canfield (2002), Calibration of sulfate levels in the archean ocean, *Science*, *298*, 2371–2374.

Habicht, K. S., L. Salling, B. Thamdrup, and D. E. Canfield (2005), Effect of low sulfate concentrations on lactate oxidation and isotope fractionation during sulfate reduction by *Archaeoglobus fulgidus* strain z, *Appl. Environ. Microbiol.*, *71*, 3770–3777.

Jørgensen, B. B. (1979), A theoretical model of the stable sulfur isotope distribution in marine sediments, *Geochim. Cosmochim. Acta*, *43*, 363–374.

Luff, R., K. Wallmann, S. Grandel, and M. Schluter (2000), Numerical modeling of benthic processes in the deep Arabian Sea, *Deep Sea Res., Part II*, *47*, 3039–3072.

Meysman, F. J. R., B. P. Boudreau, and J. J. Middelburg (2005), Modeling reactive transport in sediments subject to bioturbation and compaction, *Geochim. Cosmochim. Acta*, *69*, 3601–3617.

Middelburg, J. J., P. M. J. Herman, and C. H. R. Heip (2003), Reactive transport in surface sediments: 1. Model complexity and software quality, *Comput. Geosci.*, *29*, 291–300.

Roache, P. (1982), *Computational Fluid Dynamics*, Hermosa, Albuquerque, N. M.

Rudnicki, M. D., H. Elderfield, and B. Spiro (2001), Fractionation of sulfur isotopes during bacterial sulfate reduction in deep ocean sediments at elevated temperatures, *Geochim. Cosmochim. Acta*, *65*, 777–789.

Rysgaard, S., and P. Berg (1996), Mineralization in a northeastern Greenland sediment: Mathematical modeling, measured sediment pore water profiles and actual activities, *Aquat. Microbial Ecol.*, *11*, 297–305.

Sasowsky, I. D. (2006), Model verification and documentation are needed, *Eos Trans. AGU*, *87*(25), 248.

Soetaert, K., P. M. J. Herman, and J. J. Middelburg (1996), A model of early diagenetic processes from the shelf to abyssal depths, *Geochim. Cosmochim. Acta*, *60*, 1019–1040.

Steefel, C. I., and K. T. B. MacQuarrie (1996), Approaches to modeling of reactive transport in porous media, in *Reactive Transport in Porous Media*, *Rev. Mineral.*, vol. 34, chap. 2, pp. 83–129, Mineral. Soc. of Am., Washington, D. C.

Strang, G. (1968), On the construction and comparison of difference schemes, *SIAM J. Numer. Anal.*, *21*, 506–517.

Wijsman, J. W. M., P. M. J. Herman, J. J. Middelburg, and K. Soetaert (2002), A model for early diagenetic processes in sediments of the continental shelf of the Black Sea, *Estuarine Coastal Shelf Sci.*, *54*, 403–421.

Wortmann, U. G. (2006), A 300 m long depth profile of metabolic activity of sulfate reducing bacteria in the continental margin sediments of south Australia (ODP Site 1130) derived from inverse reaction-transport modeling, *Geochem. Geophys. Geosyst.*, *7*, Q05012, doi:10.1029/2005GC001143.

Wortmann, U. G., and B. M. Chernyavsky (2007), Impact of large scale evaporitic events on the global cycling of carbon and sulfur, *Nature*, in press.

Wortmann, U. G., M. Böttcher, and S. Bernasconi (2001), Hypersulfidic deep biosphere indicates extreme sulfur isotope fractionation during single step microbial sulfate reduction, *Geology*, *29*, 647–650.

Yeh, G. T., and V. S. Tripathi (1989), A critical evaluation of recent developments in hydrogeochemical transport models of reactive multichemical components, *Water Resour. Res.*, *25*, 93–108.

Zysset, A., and F. Stauffer (1992), Modeling of microbial processes in groundwater infiltration systems, in *Mathematical Modeling in Water Resources*, edited by T. F. Russell et al., pp. 325–332, Comput. Mech., Billerica, Mass.